

Matter Wave Diffraction from an Inclined Transmission Grating: Searching for the Elusive ^4He Trimer Efimov State

R. Brühl, A. Kalinin, O. Kornilov, and J. P. Toennies

Max-Planck-Institut für Strömungsforschung, Bunsenstr. 10, 37073 Göttingen, Germany

G. C. Hegerfeldt and M. Stoll

Institut für Theoretische Physik, Universität Göttingen, Friedrich-Hund-Platz 1, 37077 Göttingen, Germany

(Dated: August 26, 2018)

The size of the helium trimer is determined by diffracting a beam of ^4He clusters from a 100 nm grating inclined by 21° . Due to the bar thickness the projected slit width is roughly halved to 27 nm, increasing the sensitivity to the trimer size. The peak intensities measured out to the 8th order are evaluated via a few-body scattering theory. The trimer pair distance is found to be $\langle r \rangle = 1.1 + 0.4 / -0.5$ nm in agreement with predictions for the ground state. No evidence for a significant amount of Efimov trimers is found. Their concentration is estimated to be less than 6%.

PACS numbers: 33.15.-e, 03.75.Be, 21.45.+v, 36.40.Mr

In 1970 Vitali Efimov found a remarkable unexpected property in the notoriously difficult three-body problem [1]. According to Efimov a weakening of the two-body interaction in a system of three identical Bosons can lead to the appearance of an infinite number of bound levels, instead of dissociation as one would expect from classical mechanics. This effect is related to the divergence of the atomic scattering length a with decreasing binding energy E_b between two of the particles [2]. In nuclear physics, despite extensive searches, no example for the Efimov effect has been found up to now [3]. At present the most promising candidate is the ^4He trimer as first predicted by Lim, Duffy, and Damert in 1977 [4], although there have been recent attempts to identify Efimov molecules in ultracold collisions of Cs atoms [5].

Because of their very weak binding the existence of the ^4He dimer and trimer could only recently be established experimentally by a new technique involving matter-wave diffraction [6]. A beam of clusters formed in a cryogenic free jet expansion is directed at a nanostructured $d = 100$ nm period SiN_x transmission grating. Since the cluster de Broglie wave length λ is inversely proportional to the cluster number size first order Bragg diffraction peaks for different sizes are observed at different angles $\vartheta \approx \lambda/d$, thereby identifying the clusters uniquely. This technique can also be used to measure the spatial extent of the clusters. From an analysis of the ^4He dimer diffraction pattern the slit function of the grating could be determined and from this the effective slit width for passage of the dimer [7, 8]. After accounting for the velocity dependent van der Waals interaction the effective reduction of the slit width was shown to be equal to $\frac{1}{2} \langle r \rangle$, where the mean bond length was found to be $\langle r \rangle = 5.2 \pm 0.4$ nm [7]. This extremely large distance is due to the weak binding energy which was estimated to be only $|E_b| = 1.1 + 0.3 / -0.2$ mK [7].

For the helium trimer, theory predicts one Efimov state with a similarly weak binding energy of $|E_e| = 2.3$ mK in addition to the ground state with $|E_g| = 126$ mK with corresponding pair distances (bond lengths) $\langle r \rangle = 7.97$ nm and 0.96 nm, respectively [9]. Since for the trimer the slit width reduction

can be shown to be $\frac{3}{4} \langle r \rangle$ these two s -states are expected to be distinguishable by their sizes. However, experiments similar to those used for the dimer did not yield conclusive results which, ultimately, was attributed to an insufficient resolution. The present experiment overcomes this limitation by rotating the grating by an angle Θ_0 around an axis parallel to the slits as seen in Fig. 1. At $\Theta_0 = 21^\circ$, due to the thickness of the bars, the projected slit width is more than halved to $s_\perp = 26.9$ nm, providing a good compromise between the improvement in both the ratio $\langle r \rangle / s_\perp$ and the resolution at the expense of total transmission. The apparatus used is otherwise similar to the one described in detail in Ref. [10]. For the trimer measurements the cryogenic source temperatures T_0 and pressures P_0 were varied between $(T_0, P_0) = (6.7 \text{ K}, 1 \text{ bar})$ and $(40 \text{ K}, 50 \text{ bar})$ to produce optimal trimer mole fractions of up to 7% [11]. The collimated beam with a velocity spread $\Delta v/v \leq 2\%$ has a spatial lateral coherence greater than the exposed 100 grating slits. For both atom and trimer measurements the mass spectrometer detector was set at the $^4\text{He}^+$ ion mass. The maximum trimer signal was about 200 counts/sec.

Figure 2a shows a diffraction pattern out of a series of altogether 13 taken for various velocities at $\Theta_0 = 18^\circ$ and 21° . The most intense peaks are due to helium atoms while those marked by circles belong to trimers. Whereas in the past the diffraction intensities I_n for all orders n had been found to be perfectly symmetric ($I_n = I_{-n}$), a careful inspection of the new peak intensities in Fig. 2b exhibits an up to 10% deviation from symmetry [12]. This new feature is clearly demonstrated by the contrast $C_n = (I_n - I_{-n}) / (I_n + I_{-n})$ displayed in Fig. 2c. By modifying the diffraction theory of Ref. [13] to account for the asymmetry the new measurements could be evaluated to obtain the bond length of the helium trimer $\langle r \rangle = 1.1 + 0.4 / -0.5$ nm. Assuming the theoretical values of $\langle r \rangle$ the maximum concentration of Efimov trimers in the beam is estimated to be less than 6%. Although their small concentration may possibly be explained by collisional depletion in the expansion, the negative result obviously also raises new doubts about the existence of an Efimov state in $^4\text{He}_3$.

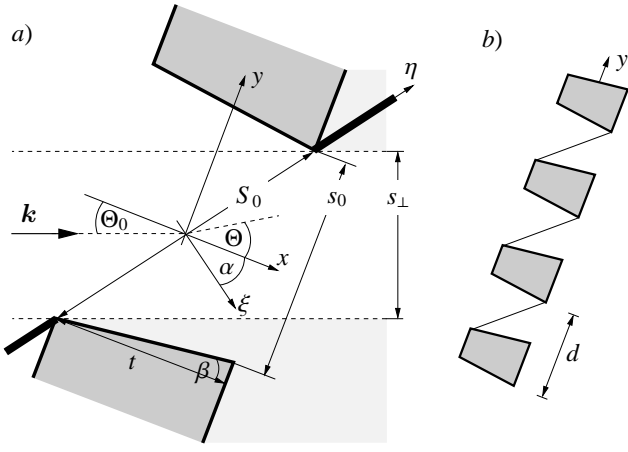


FIG. 1: Diffraction geometry at non-normal incidence: *a*) A single slit of width s_0 in a plate of thickness t with a wedge angle β has a projected slit width of s_{\perp} . Both the angle of incidence Θ_0 and the angle Θ are measured relative to the plate normal. The hypothetical thin plate drawn along the η direction with a slit of width $S_0 = \sqrt{(s_0 + t \tan \beta)^2 + t^2}$ at an angle $\alpha = \arcsin(t/S_0)$ relative to the thick plate along the y direction casts the same geometrical shadow as the thick plate. *b*) Transmission grating of period d along the y direction.

From atom beam transmission experiments [10] the grating bars are found to have a thickness $t = 118.3 \pm 0.5$ nm and their inner faces have a wedge angle $\beta = 6.7 \pm 0.5^\circ$ with the direction perpendicular to the grating (Fig. 1). Since the angle of inclination (angle of incidence) Θ_0 exceeds the wedge angle β the upper bar faces (Fig. 1) are shadowed by the front edges of the bars. Obviously in this geometry the opening (s_0 in Fig. 1) used in previous calculations of the scattering amplitude for normal incidence [7, 8] is no longer appropriate. Instead the slit is modeled by a diagonal opening of width S_0 in a thin plate along the η axis (Fig. 1) which casts the same geometrical shadow as the original slit [14]. Complications from scattering from the upper bar faces are not expected since the cluster de Broglie wave length $\lambda \approx 1 \text{ \AA}$ is much smaller than the slit width such that the diffraction is concentrated in a small range of angles of the order of $\vartheta = \Theta - \Theta_0 \approx \lambda/s_{\perp} \approx 2^\circ$, much smaller than $\Theta_0 - \beta \approx 14^\circ$. Modeling the incident beam by a plane wave of wave vector \mathbf{k} with $k = |\mathbf{k}| = 2\pi/\lambda$ and imposing Kirchhoff boundary conditions along the slit S_0 leads to the following expression for the scattering amplitude of the diagonal slit [8, 15]

$$f_{\text{slit}}(\Theta) = \frac{\cos(\Theta_0 + \alpha)}{\sqrt{\lambda}} \int_{-S_0/2}^{S_0/2} d\eta e^{-iK(\Theta)\eta} \tau(\eta), \quad (1)$$

where the bar thickness enters through $\sin \alpha = t/S_0$ and

$$K(\Theta) = k [\sin(\Theta + \alpha) - \sin(\Theta_0 + \alpha)] \quad (2)$$

is the wave vector transfer along the slit direction (η axis). The transmission function $\tau(\eta)$ in Eq. (1) accounts for the size of the cluster [7] as well as the weak van der Waals surface

interaction of the form $-C_3/l^3$ between the atoms and the bar material [8], where l is the distance from the surface.

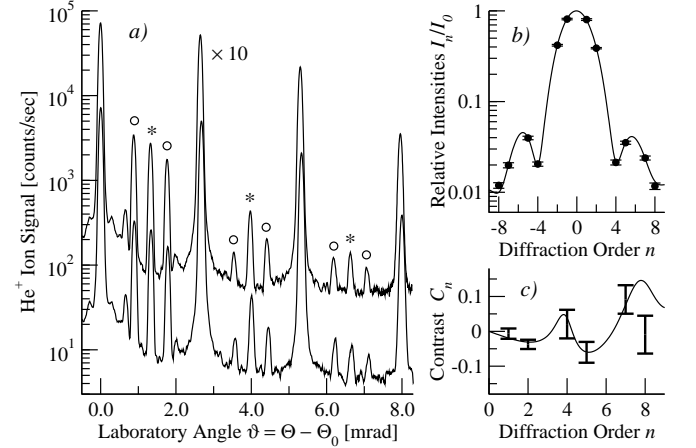


FIG. 2: *a*) ^4He diffraction pattern at $\Theta_0 = 21^\circ$ angle of incidence measured for the source conditions $(T_0, P_0) = (16.5 \text{ K}, 7.0 \text{ bar})$ corresponding to a trimer de Broglie wavelength of $\lambda = 0.83 \text{ \AA}$. The signal at negative diffraction angles has been shifted upwards by a factor 10 and mirrored onto the positive side for comparison. The trimer diffraction peaks are marked by circles, dimer peaks by stars. *b*) Relative trimer peak intensities I_n/I_0 . *c*) Corresponding contrast $C_n = (I_n - I_{-n})/(I_n + I_{-n})$. The curves in *b*) and *c*) are best-fit calculations based on Eq. (6).

The inclined transmission grating consists of many slits aligned along the y axis with period d (Fig. 1b). The periodicity then gives rise to sharp principal diffraction maxima located at the Bragg angles Θ_n satisfying

$$k [\sin \Theta_n - \sin \Theta_0] = 2\pi n/d \quad (3)$$

for $n = 0, \pm 1, \pm 2$, etc [16]. Solving Eq. (3) for Θ_n and inserting into Eq. (2) yields $K(\Theta_n)$ at which the scattering amplitude determining the intensity of the n -th diffraction order is to be evaluated. By expanding through second order in n , $K(\Theta_n)$ can be expressed as

$$\frac{K(\Theta_n)}{\cos(\Theta_0 + \alpha)} \approx \frac{2\pi n}{d \cos \Theta_0} + \lambda \frac{\tan \Theta_0 - \tan(\Theta_0 + \alpha)}{4\pi} \left(\frac{2\pi n}{d \cos \Theta_0} \right)^2.$$

Thus, although the scattering amplitude itself is even under the change of the sign of $K(\Theta)$, it is probed at a wave vector transfer for which $K(\Theta_n) \neq -K(\Theta_{-n})$. The origin of the experimentally observed asymmetry $I_n \neq I_{-n}$ of the diffraction pattern lies, therefore, in the non-alignment of the slits S_0 (η axis) and the direction of periodicity (y axis). The asymmetry decreases with λ because for a smaller de Broglie wave length less clusters are diffracted into the shaded region of the slits (Fig. 1). Clearly, for $\alpha = 0$ (thin grating) the symmetric case is recovered. Supplementary calculations indicate that the van der Waals surface interaction has only a minor effect on the asymmetry.

An analytical expression for the relative diffraction intensities I_n/I_0 is obtained by introducing the functions $\Phi^\pm(K)$ and

$\Phi^-(K)$ [8]

$$\Phi^\pm(K) = \int_0^{S_0/2} d\eta e^{\pm iK\eta} \frac{\frac{\partial}{\partial \eta} \tau[\pm(S_0/2 - \eta)]}{\tau(0)} \quad (4)$$

which allows the scattering amplitude to be expressed exactly as

$$f_{\text{slit}}(\Theta) = \frac{\cos(\Theta + \alpha)}{\sqrt{\lambda}} \tau(0) \times \frac{e^{iK(\Theta)S_0/2}\Phi^-(K(\Theta)) - e^{-iK(\Theta)S_0/2}\Phi^+(K(\Theta))}{iK(\Theta)}. \quad (5)$$

To conveniently combine the functions $\Phi^\pm(K)$ with the exponentials in Eq. (5) their logarithms are expanded in a power series: $\ln \Phi^\pm(K) = \sum_{j=1}^{\infty} (\pm iK)^j R_j^\pm / j!$, which uniquely defines the complex numbers R_j^\pm known as the cumulants. For example, the first cumulants are given by $R_1^\pm = \pm \int_0^{\pm S_0/2} d\eta [1 - \tau(\eta)]$ and account for the different transmission in the two halves of the slit. For the diffraction orders $|n| \lesssim 8$ encountered experimentally it is sufficient to retain only the first two terms of this expansion. Inserting them into Eq. (5) the n -th order diffraction intensity becomes, to good approximation,

$$\frac{I_n}{I_0} = \frac{e^{-K(\Theta_n)^2 \Sigma^2} e^{-K(\Theta_n)\Gamma}}{\left(\frac{K(\Theta_n)\sqrt{S_{\text{eff}}^2 + \Delta^2}}{2}\right)^2} \left[\sin^2\left(\frac{K(\Theta_n)S_{\text{eff}}}{2}\right) + \sinh^2\left(\frac{K(\Theta_n)\Delta}{2}\right) \right]. \quad (6)$$

Here, the effective slit width $S_{\text{eff}} = S_0 - \text{Re}(R_1^+ + R_1^-)$ accounts for the reduction of the geometrical slit width S_0 due to the surface interaction as well as the finite cluster size. The exponential involving $\Sigma = \sqrt{\text{Re}(R_2^+ + R_2^-)}/2 \approx 5$ nm includes the Debye-Waller attenuation due to irregular variations of the slit width across the grating and also accounts for cluster breakup [7, 8]. The surface interaction removes the intensity zeros through the term involving $\Delta = \text{Im}(R_1^+ + R_1^-) \approx 10$ nm and contributes weakly to the asymmetry through $\Gamma = \text{Im}(R_1^+ - R_1^-) \approx 1.5$ nm.

Experimental values for S_{eff} were obtained from fits of the intensity formula Eq. (6) to trimer diffraction patterns (Fig. 2b) measured for $T_0 = 6.7 - 40$ K. In Fig. 3 the projected effective slit widths $s_{\perp \text{eff}} = S_{\text{eff}} \cos(\Theta_0 + \alpha)$ for ${}^4\text{He}$, ${}^4\text{He}_2$ and ${}^4\text{He}_3$ at $\Theta_0 = 21^\circ$ are plotted as functions of the beam velocity. The atom data were used to determine, along the lines of Ref. [8], the projected slit width $s_{\perp} = 26.92 \pm 0.02$ nm and the van der Waals interaction coefficient was taken as $C_3 = 0.113 \pm 0.02$ meV nm³ [8]. As seen from Fig. 3 the trimer size effect at a velocity of 0.64 km/s is of the order of only 1.2 nm, clearly smaller than the 2.5 nm for the dimer. Moreover, the dimer curve runs almost parallel to the atom curve suggesting that, due to the extent of the dimer wave function, on average only one of its atoms is interacting with the surface. In contrast, the steeper slope of the trimer curve indicates the contribution of more than one atom, also confirming the relative compactness of this cluster.

The smallness of the trimer binding energy as compared to its kinetic energy allows an extension of the quantum mechanical few-body scattering approach of Ref. [13], which is based on the AGS equations [17] and originally designed to describe dimer diffraction, to treat also the trimer case. It turns out that, as a generalization of the dimer result, the size effect is caused by the width of the trimer perpendicular to its incident direction. For the dimer [7] this width can be expressed by the expectation value $\langle |r_{\perp}| \rangle = \langle r \rangle / 2$ where r denotes the dimer bond length and $|r_{\perp}|$ is its perpendicular projection (lower inset in Fig. 3). The analogous expression for the trimer, which is more intricate due to the third atom, is given by $(|r_{\perp}| + |r'_{\perp}| + |r''_{\perp}|)/2$ where the three distances are defined in the upper inset of Fig. 3. For the homonuclear ${}^4\text{He}_3$ the expectation value of this quantity reduces to $3\langle |r_{\perp}| \rangle / 2$. Moreover, since the pair interactions are dominated by the shallow s -wave dimer state, the homogeneous Faddeev equations [18] can be used to express the width in terms of the trimer bond length as $3\langle r \rangle / 4$. The complete expression for $s_{\perp \text{eff}}$, which includes the surface interaction, is then found to be

$$s_{\perp \text{eff}} = s_{\perp} - \frac{3}{4} \langle r \rangle - \zeta \text{Re} \times \left\{ \int_0^{S_0/2} d\eta \left[1 - \tau_{\text{at}}(\eta) \tau_{\text{at}}\left(\eta - \frac{1}{2} \frac{\langle r \rangle}{\zeta}\right) \tau_{\text{at}}\left(\eta - \frac{5}{8} \frac{\langle r \rangle}{\zeta}\right) \right] + \int_{-S_0/2}^0 d\eta \left[1 - \tau_{\text{at}}(\eta) \tau_{\text{at}}\left(\eta + \frac{1}{2} \frac{\langle r \rangle}{\zeta}\right) \tau_{\text{at}}\left(\eta + \frac{5}{8} \frac{\langle r \rangle}{\zeta}\right) \right] \right\}. \quad (7)$$

where $\zeta = \cos(\Theta_0 + \alpha)$ was used. The term in curly braces in Eq. (7) accounts for the surface interaction via the atom transmission functions $\tau_{\text{at}}(\eta)$ [8]. As seen in Fig. 3 this term varies between 2–4 nm in the experimental range of 0.25 – 0.64 km/s.

Using Eq. (7) the best fit curve for the trimer based on seven diffraction patterns taken at $\Theta_0 = 21^\circ$ was obtained for the bond length $\langle r \rangle = 1.0 + 0.5 / -0.7$ nm. A second series of six diffraction patterns taken at $\Theta_0 = 18^\circ$ yielded $\langle r \rangle = 1.2 + 0.5 / -0.8$ nm which confirms, within the error bars, the reproducibility of the result. The average of both results, $\langle r \rangle = 1.1 + 0.4 / -0.5$ nm, agrees well with the theoretical prediction of 0.96 nm [9] for the ${}^4\text{He}_3$ ground state. Moreover, it rules out a significant concentration of the Efimov state in the beam. With the theoretical values for $\langle r \rangle$ a simulation of the diffraction pattern for various concentrations indicates that the upper experimental limit is consistent with less than 6% Efimov trimers, reducing substantially the previous value of 15% [19].

Dedicated calculations for the formation of excited state clusters during the beam expansion are not available. Applying, for an estimate, the equilibrium model of Ref. [11] the ratio of Efimov to ground state trimers is expected to be approximately proportional to $\exp(-|E_g - E_c|/k_B T_{\infty})$. At an asymptotic temperature in the fully expanded beam of $T_{\infty} = 1 - 5$ mK in the present experiment, this is indeed a very small number ($< 10^{-11}$). The validity of this estimate, however, depends

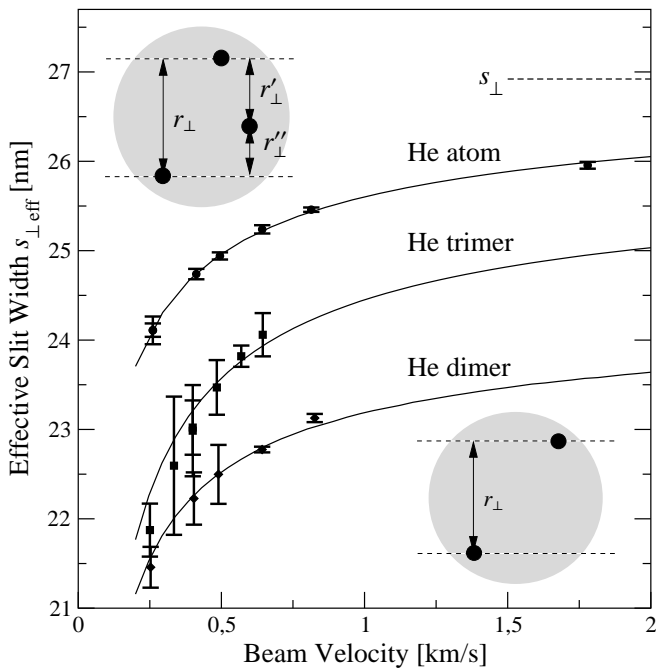


FIG. 3: Projected effective slit widths $s_{\perp,\text{eff}} = S_{\text{eff}} \cos(\Theta_0 + \alpha)$ measured at different beam velocities at an angle of incidence $\Theta_0 = 21^\circ$ for ${}^4\text{He}$, ${}^4\text{He}_2$ and ${}^4\text{He}_3$. The curves represent best fits of Eq. (7) for ${}^4\text{He}_3$ and analogous expressions for ${}^4\text{He}$ and ${}^4\text{He}_2$. Their high velocity limits are given by s_{\perp} for ${}^4\text{He}$, by $s_{\perp} - \frac{1}{2}\langle r \rangle$ for ${}^4\text{He}_2$, and by $s_{\perp} - \frac{3}{4}\langle r \rangle$ for ${}^4\text{He}_3$. The insets illustrate the “widths” traced out by the clusters along their flight paths (see text).

on the temperature at which the internal states equilibrate, which may be much larger than T_{∞} . While the collisional de-excitation of an Efimov trimer into the ground state is expected to be small [20] a realistic calculation would need to take into account the inelastic cross-section between the Efimov trimer and the co-expanding atoms. Indirect evidence for the likely robustness of the Efimov cluster comes only from the large mole fraction of the even more weakly bound ${}^4\text{He}_2$ [7].

There is, of course, also the possibility that the ${}^4\text{He}_3$ Efimov state does, in fact, not exist despite the over 40 publications which have appeared since 1977. Since all calculations have been carried out for adiabatic two-body potentials, which have been tested both experimentally [7] and by numerical methods [21], it is still conceivable that the presence of the Efimov state is affected by the sum of so far neglected small corrections to the potentials, such as a three-body contribution to the interaction [22], retardation or non-adiabatic effects [23]. For example, Gdanitz [23] showed that the latter can modify the scattering length by about 5–10%. However, a solution of the Faddeev equations based on a separable potential, which was adjusted to reproduce exactly the scattering length and the effective range of the He-He interaction, reveals that such a modification alone cannot render the Efimov state unbound.

In future experiments a promising approach to detect Efi-

mov ${}^4\text{He}_3$ could involve sampling the sizes of clusters effusing from a Knudsen cell, thereby ruling out collisional de-excitation. Then the Efimov and ground state molecules would have small but nearly equal concentrations. To compensate for the loss in signal the trimer mole fraction could be increased by going to a much higher P_0 while reducing the orifice diameter. A new, much more sensitive detector currently under development may make such experiments possible.

We are indebted to T. Savas for providing the transmission grating and thank T. Köhler for stimulating discussions.

-
- [1] V. Efimov, Phys. Lett. **33B**, 563 (1970).
 - [2] J. Lekner, Mol. Phys. **23**, 619 (1972).
 - [3] A. S. Jensen, K. Riisager, D. V. Fedorov, and E. Garrido, Rev. Mod. Phys. **76**, 215 (2004).
 - [4] T. K. Lim, S. K. Duffy, and W. C. Damert, Phys. Rev. Lett. **38**, 341 (1977).
 - [5] C. Chin, V. Vuletic, A. J. Kerman, and S. Chu, Nucl. Phys. **A684**, 641c (2001).
 - [6] W. Schöllkopf and J. P. Toennies, Science **266**, 1345 (1994).
 - [7] R. E. Grisenti, W. Schöllkopf, J. P. Toennies, G. C. Hegerfeldt, T. Köhler, and M. Stoll, Phys. Rev. Lett. **85**, 2284 (2000).
 - [8] R. E. Grisenti, W. Schöllkopf, J. P. Toennies, G. C. Hegerfeldt, and T. Köhler, Phys. Rev. Lett. **83**, 1755 (1999).
 - [9] P. Barletta and A. Kievsky, Phys. Rev. A **64**, 042514 (2001). A. K. Motovilov, W. Sandhas, S. A. Sofianos, and E. A. Koganova, Eur. Phys. J. D **13**, 33 (2001). E. Braaten and H.-W. Hammer, Phys. Rev. A **67**, 042706 (2003).
 - [10] R. E. Grisenti, W. Schöllkopf, J. P. Toennies, J. R. Manson, T. A. Savas, and H. I. Smith, Phys. Rev. A **61**, 033608 (2000).
 - [11] L. W. Bruch, W. Schöllkopf, and J. P. Toennies, J. Chem. Phys. **117**, 1544 (2002).
 - [12] As seen in Fig. 2 the diffraction angles $\vartheta_n = \Theta_n - \Theta_0$ are also asymmetric ($\vartheta_n \neq -\vartheta_{-n}$) in agreement with the Bragg law Eq. (3). However, this effect is unrelated to the intensity asymmetry.
 - [13] G. C. Hegerfeldt and T. Köhler, Phys. Rev. A **57**, 2021 (1998). G. C. Hegerfeldt and T. Köhler, Phys. Rev. A **61**, 23606 (2000).
 - [14] This argument can also be derived formally from diffraction theory under the condition $\lambda \ll t, S_0$. See, e.g., P. M. Morse and H. Feshbach, *Methods of Theoretical Physics* (McGraw-Hill, New York, 1953), §11.4, p. 1551.
 - [15] M. Born and E. Wolf, *Principles of Optics* (Pergamon Press, London, 1959), §11.3.
 - [16] For $n2\pi/(kd) \ll 1$ one has $\vartheta_n = \Theta_n - \Theta_0 \approx n2\pi/(kd \cos \Theta_0)$, as used in Ref. [10].
 - [17] E. O. Alt, P. Grassberger, and W. Sandhas, Nucl. Phys. B **2**, 167 (1967).
 - [18] A. G. Sitenko, *Lectures in Scattering Theory* (Pergamon Press, 1971).
 - [19] A. Kalinin, O. Kornilov, L. Rusin, J. P. Toennies, and G. Vladimirov, Phys. Rev. Lett. **93**, 163402 (2004).
 - [20] G. C. Hegerfeldt and T. Köhler, Phys. Rev. Lett. **84**, 3215 (2000).
 - [21] J. B. Anderson, J. Chem. Phys. **120**, 9886 (2004).
 - [22] I. Røeggen and J. Almlöf, J. Chem. Phys. **102**, 7095 (1995).
 - [23] R. J. Gdanitz, Mol. Phys. **99**, 923 (2001).